9th Asia-Pacific Conference on Wind Engineering
Auckland, New Zealand
3-7 December 2017

Study on multiple definitions of mean wind speed in pedestrian wind environment analyses using LES

H. Kikumoto[1], R. Ooka[1], M. Han[2] and K. Nakajima[2]

[1]Institute of Industrial Science
The University of Tokyo, Tokyo, Japan

[2]Department of Architecture, Graduate School of Engineering
The University of Tokyo, Tokyo, Japan

Abstract

When analyzing the pedestrian wind environment, the evaluated mean wind speed varies in its definition depending on the method used, such as in wind tunnel experiments and in computational fluid dynamics (CFD) analyses. This study, first, defined three types of mean wind speed (mean-vector speed, mean speed, and effective speed) and analytically investigated how they relate to each other. Secondly, the discrepancies between the three mean wind speeds were quantitatively analyzed by conducting a large-eddy simulation (LES) of flow around a single building model in an urban boundary layer. In the vicinity of the ground surface, the difference between the mean wind speeds became larger in the recirculation flow near the building's windward corners and in the wake of the building. However, in the region where the maximum wind speeds occurred, all the mean wind speeds displayed values very close to each other. Finally, we presented methods to estimate mean speed using information that can be obtained from CFD with RANS (Reynolds-averaged Navier–Stokes) equations-type turbulence models. By modeling the probability distribution of the instantaneous velocity vector in a multivariate Gaussian distribution, we demonstrated its ability to estimate the mean speed with high accuracy.

1. Introduction

The pedestrian wind environment (PWE) in cities has been most commonly analyzed using wind tunnel experiments (WTEs). However, along with the recent advances in computing power, the number of studies applying computational fluid dynamics (CFD) has been increasing.

A variety of wind speed measurement techniques exist in WTEs. Nevertheless, when measuring wind speed in an actual city model with a complicated shape, an omnidirectional anemometer, such as a thermistor anemometer, is generally preferred considering its lower cost and the robustness of the sensor.

In recent CFD literature, highly accurate turbulence models, such as large-eddy simulations (LES), are increasingly being used in studies. However, owing to its lower computational cost and ease in handling the model, the practical analysis of the PWE is still generally using RANS (Reynolds-averaged Navier–Stokes) equations-type turbulence models.

In the both WTEs and CFDs, "mean wind speed" is used as an indicator in PWE analysis. Yet, the definition of mean wind speed in WTE with an omnidirectional anemometer does not precisely match the one used in CFD with an RANS-type turbulence model (CFD (RANS)) [1]. Although both WTE and CFD have their inherent measurement and prediction error factors, when analyzing the PWE it is necessary to be consistent regardless of the method employed. In addition, when evaluating the prediction accuracy of CFD with data from WTE, it is a prerequisite that the indicators being compared are of the same physical quantity.

In this study, we first defined mean wind speed with multiple different definitions and analytically investigated how they relate to each other. Secondly, we investigated the discrepancies between those wind speeds quantitatively by conducting a LES for flow around a single building model in an urban boundary layer. Moreover, using the results of the LES, we studied methods to estimate the mean wind speed obtained by omnidirectional anemometer using statistics from CFD (RANS) results.

2. Multiple definitions of mean wind speed

The instantaneous wind velocity in the three-dimensional space is represented by $\mathbf{u}$. The Reynolds-average and deviation from the mean of a quantity are denoted by $\langle\bullet\rangle$ and $\bullet'$ respectively. In other words, $\mathbf{u} = \langle\mathbf{u}\rangle + \mathbf{u}'$. The square norm of a vector is expressed by $\|\bullet\|$. This defines the instantaneous wind speed as $s \equiv \|\mathbf{u}\| = \left(\mathbf{u}^{\mathrm{T}}\mathbf{u}\right)^{0.5}$. Here, T of the vector right shoulder means the transpose of the vector.

We define three types of mean wind speed: mean-vector speed, V_{mv}, mean speed, V_{ms}, and effective speed, V_{es}, as follows.

$$V_{\mathrm{mv}} \equiv \|\langle\mathbf{u}\rangle\| = \left(\langle\mathbf{u}\rangle^{\mathrm{T}}\langle\mathbf{u}\rangle\right)^{0.5} = (2K)^{0.5} \tag{1a}$$

$$V_{\mathrm{ms}} \equiv \langle\|\mathbf{u}\|\rangle = \langle s\rangle \tag{1b}$$

$$V_{\mathrm{es}} \equiv \langle\|\mathbf{u}\|^2\rangle^{0.5} = \langle s^2\rangle^{0.5} = (2K + 2k)^{0.5} \tag{1c}$$

Here, K and k are the kinetic energies of the mean flow and turbulence respectively.

Method	V_{mv}	V_{ms}	V_{es}
WTE*		✓	
CFD (RANS)	✓		✓
CFD (LES)	✓	✓	✓**

Table 1. Analysis methods and mean wind speeds to be evaluated. * With omnidirectional anemometer; ** Approximated value because of the spatial filtering of small-scale turbulence in the LES.

The omnidirectional anemometer in WTEs measures the s as instantaneous speed data. Although the measured value is temporally filtered by the thermal inertia of its sensor probe, the mean wind speed as a result of time-averaging the data is the same as the V_{ms}. In the case of CFD (RANS), the typically

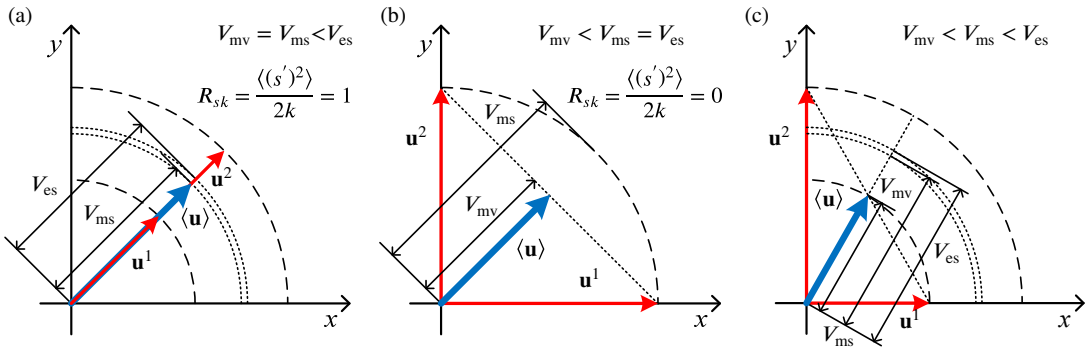

Figure 1. Schematic diagram of the relationship of V_{mv}, V_{ms} and V_{es} showing an example with two instantaneous velocity vectors $\mathbf{u}^1$ and $\mathbf{u}^2$. $\langle \mathbf{u} \rangle = 0.5(\mathbf{u}^1 + \mathbf{u}^2)$. There are three cases with (a) constant direction, (b) constant length and (c) otherwise.

evaluated mean wind speed is V_{mv}. It is also possible to evaluate the V_{es} from the sum of the kinetic energies of the mean flow and turbulence. Table 1 shows the mean wind speeds that can be evaluated using the WTE or CFD methods, and the inconsistency between WTE and CFD (RANS).

3. Relationship between mean wind speeds

$V_{ms}^2 - V_{mv}^2 = \langle s \rangle^2 - 2K = 2k - \langle (s')^2 \rangle$. The following equation is obtained based on the facts that $\langle (s')^2 \rangle \geq 0$ and that any mean wind speed is positive.

$$V_{ms} = \left(V_{mv}^2 + 2k - \langle (s')^2 \rangle \right)^{0.5} \leq \left(V_{mv}^2 + 2k \right)^{0.5} = V_{es} \qquad (2)$$

Although proof cannot be demonstrated here owing to limited space, the henceforth relationship follows.

$$V_{ms} - V_{mv} = \langle \|\mathbf{u}\| \rangle - \|\langle \mathbf{u} \rangle\| \geq 0 \qquad (3)$$

To summarize the above, the following relationships between the mean wind speeds is obtained.

$$V_{mv} \leq V_{ms} \leq V_{es} \text{ or } 2K \leq \langle s \rangle^2 \leq 2K + 2k = \langle s^2 \rangle \qquad (4)$$

Further, by substituting $\langle s \rangle^2 - 2K = 2k - \langle (s')^2 \rangle$ into Eq. (4) and defining $R_{sk} \equiv \langle (s')^2 \rangle / 2k$, R_{sk} is in the following range.

$$0 \leq R_{sk} \leq 1 \qquad (5)$$

Regarding the difference between the mean wind speeds, k imposes a limit on the maximum extent (Eq. (4)). Therefore, at a point where turbulence has a relatively small kinetic energy compared with that of the mean flow, the mean wind speed is expected to result in very close values using any of the three definitions.

On the other hand, at a point of a k magnitude that is large, differences between the mean wind speeds can occur. Disturbances to velocity can change the length and direction of the instantaneous velocity vector. Even if the vector length is changed by disturbance, $V_{ms} = V_{mv}$ when its direction is constant (Fig. 1 (a)). Conversely, even if there is change in the direction of the vector, $\langle (s')^2 \rangle = 0$ when the length is constant, and $V_{ms} = V_{es}$ based on Eq. (2) (Fig. 1 (b)).

However, in the real airflow occurring in cities, a situation where the length or direction remain constant in all velocity samples is less likely to occur. As a result, wind velocity is in an intermediate state of the above two extreme cases, and V_{ms} does not exactly match with any of V_{mv} or V_{es} (Fig. 1 (c)). The relative impact of the change in the length and direction of velocity is represented in short by the value of R_{sk}.

4. Background on the case study using LES

We carried out a LES corresponding to a benchmark case (2:1:1 shape building model) in the CFD guidebook provided by the Architectural Institute of Japan [2]. Table 1 and Figure 2 show analysis conditions and the analysis domain of the performed LES. The coordinate origin was set at the center point of the building on the ground surface. An additional LES simulating flow in an environmental wind tunnel in the Institute of Industrial Science of The University of Tokyo was conducted to generate inflow turbulence for the main analysis domain. The results in this paper were normalized with the height of the building model H (= 0.32 m) and the mean inflow velocity at the same height U_{ref} (= 4.385 m/s). V_{mv}, V_{ms} and V_{es} were evaluated using the LES results.

Item	Content
Code	OpenFOAM v2.1.1
Sub-grid scale model	Standard Smagorinsky model (C_s = 0.12) with van Driest damping function
Analysis domain	10.75 H (x) × 6.875 H (y) × 5.625 H (z)
Time step	0.001 s
Time marching	PISO
Time discretization	Euler-implicit
Space discretization	2nd-order central difference
Inflow B.C.	Inflow turbulence data obtained from an additional LES which simulated urban boundary layer flow in a wind tunnel
Outflow B.C.	Gradient-zero
Wall B.C.	Spalding's law

Table 2. Analysis conditions of LES.

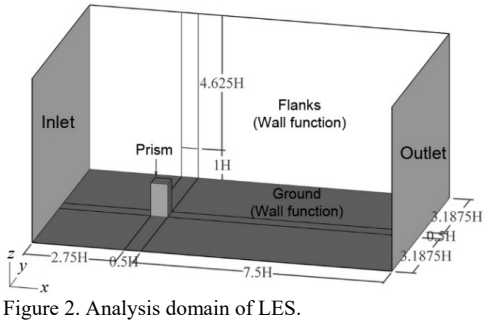

Figure 2. Analysis domain of LES.

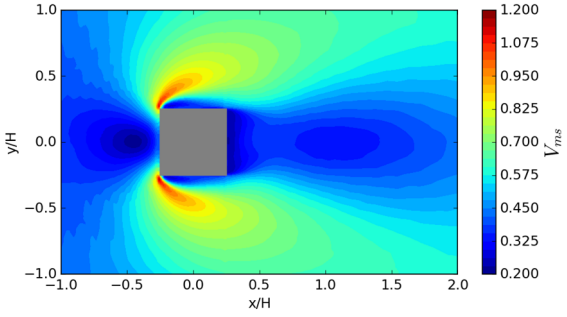

Figure 3. Distribution of V_{ms} at z/H = 1/16.

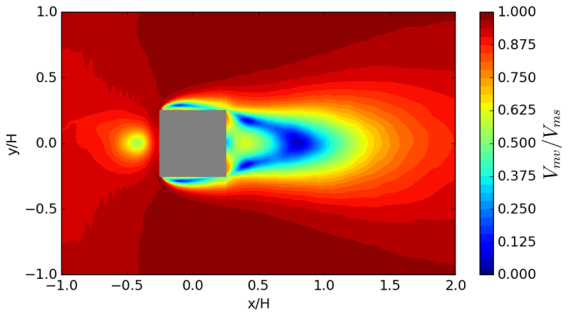

(a)

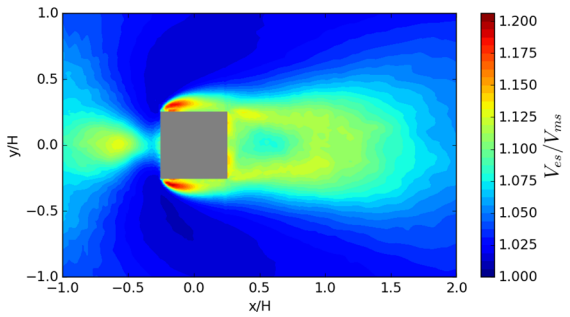

(b)

Figure 4. Ratio between mean wind speeds at $z = H/16$. (a) V_{mv}/V_{ms}, (b) V_{es}/V_{ms}.

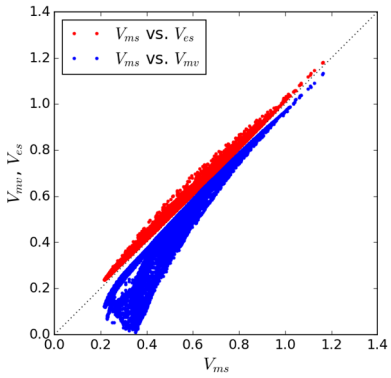

Figure 5. Scatter plot between mean wind speeds in the range of $-1 < x/H < 2$, $-1 < y/H < 1$ and $z/H = 1/16$.

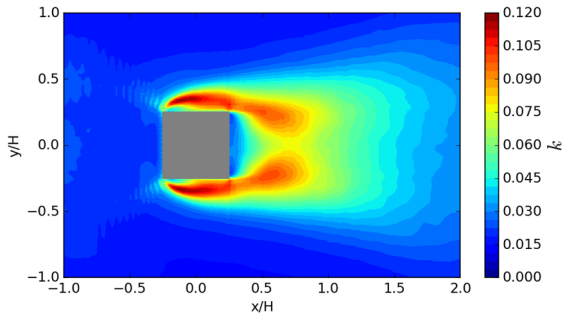

Figure 6. Distribution of k at $z/H = 1/16$.

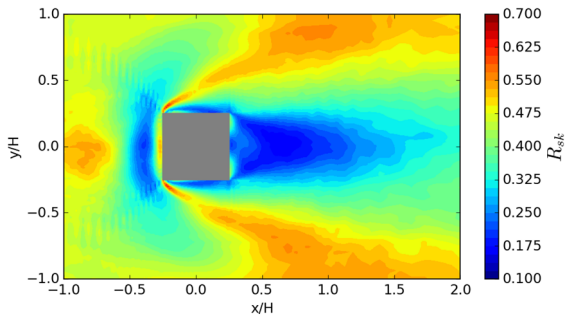

Figure 7. Distribution of R_{sk} at $z/H = 1/16$.

5. Results of the case study using LES

Tominaga et al. (2008) have studied the flow field formed around the same building model in this analysis in detail [3]. In this paper, from the viewpoint of the PWE, we examine data in the horizontal plane of $z = 1/16H$, which is relatively close to the ground surface.

Figure 3 shows the distribution of mean speed V_{ms}. The other mean wind speeds are presented in Fig. 4, which are normalized by V_{ms}. Furthermore, Fig. 5 shows the scatter of V_{ms} in relation to V_{mv}, and V_{ms} in relation to V_{es} at each point of the area under consideration.

The relationship $V_{mv} \leq V_{ms} \leq V_{es}$, which has been analytically shown in the Section 3, was also seen in the results of the LES. The inconsistency between the three mean wind speeds became larger in the wake of the building and in the recirculating flow near the windward corners of the building. V_{mv} / V_{ms} varied from almost 0 to 1, whereas V_{es} / V_{ms} is in the range of 1.0-1.2 (Fig. 4). In other words, V_{ms} tended to be closer to V_{es} than V_{mv} on average. In addition, Fig. 5 shows that the difference between V_{ms} and V_{mv} grows larger as V_{ms} becomes smaller. V_{mv} approaches V_{ms} at a point where wind speed was maximum. On the other hand, the difference between V_{ms} and V_{es} grows large for intermediate mean speeds. However, V_{es} also approaches V_{ms} as wind speed becomes larger.

Figures 6 and 7 show distributions of turbulence kinetic energy, k, and the ratio of variance of speed to $2k$, $R_{sk}(= \langle (s')^2 \rangle / 2k)$, respectively. k corresponds to the maximum magnitude of discrepancy between the mean wind speeds (difference between V_{es} and V_{mv}). R_{sk} represents the relative degree of change in the length and direction of the wind velocity vector due to the turbulence. When the velocity vector is more significantly affected by the change in direction than by the change in length, R_{sk} is close to 0 and V_{ms} is close to V_{es}. Conversely, when R_{sk} is close to 1, V_{ms} is close to V_{mv}.

In the recirculating flow near the windward corners of the building, k became the largest and R_{sk} had intermediate values. As a result, in such locations the difference between V_{ms} and V_{mv}, and V_{ms} and V_{es} was large. However, in the locations where the maximum wind speed was present just outside the recirculation flow, k was relatively small with respect to the kinetic energy of the mean flow, and the three mean wind speeds demonstrated very similar values.

In the wake of the building, R_{sk} displayed small values while k maintained relatively large values. This is because, in this region, the length of the instantaneous velocity vector displays relatively little change, in contrast to its direction which changes greatly. As a result, the difference between V_{ms} and V_{mv} became particularly large. This is consistent with the fact that the results of the mean wind speed of CFD (RANS) differed greatly from those of WTE in the wake of the building, where wind becomes weaker, as pointed out in the CFD guide book [2]. In the guide book, a method for correcting the mean wind speed in CFD (RANS) by incorporating the effect of k is proposed. However, the method gives V_{es} as the estimate of V_{ms}, which in principle tends to result in an overestimation of V_{ms}.

6. Possible methods to estimate V_{ms}

CFD (RANS) is not able to directly analyze V_{ms} or s statistics. However, the mean velocity vector $\langle \mathbf{u} \rangle$ and the covariance matrix of velocity fluctuation $\langle \mathbf{u}'(\mathbf{u}')^{\mathrm{T}} \rangle$ $(= (\langle u_i' u_j' \rangle))$ can be obtained from the analysis. We discuss here two estimation methods of V_{ms} from the parameters above, using the results of LES.

Method 1: Velocity fluctuation in the direction of mean velocity vector

We suppose that the variance of speed, $\langle (s')^2 \rangle$, can be approximated by the velocity variance in the direction of the mean velocity vector, $\langle (v')^2 \rangle$. By using the unit vector in the direction of the mean velocity vector, $\mathbf{e}^*$ $(= (e_i^*) = \langle \mathbf{u} \rangle / \| \langle \mathbf{u} \rangle \|)$, $\langle (v')^2 \rangle$ is evaluated using the following equation.

$$\langle (v')^2 \rangle = \sum_{i=1}^{3} \sum_{j=1}^{3} e_i^* e_j^* \langle u_i' u_j' \rangle \tag{6}$$

Replacing $\langle (s')^2 \rangle$ with $\langle (v')^2 \rangle$ in Eq. (2), this method gives an estimate of V_{ms}, $V_{\mathrm{ms,v}}$, as follows.

$$V_{\mathrm{ms,v}} = \left[V_{\mathrm{mv}}^2 + 2k - \langle (v')^2 \rangle \right]^{0.5} \tag{7}$$

Method 2: Modeled probability density function of the instantaneous velocity vector

Using the original meaning of V_{ms} as $\langle s \rangle$, it also can be represented by the following expression using the probability density function of the instantaneous velocity vector, $f(\mathbf{u})$.

$$V_{\mathrm{ms}} = \int_{\Omega} s f(\mathbf{u}) \mathrm{d}\mathbf{u} \tag{8}$$

Here, Ω is the space where $\mathbf{u}$ is defined. Generally, the precise form of $f(\mathbf{u})$ can not be known using CFD (RANS). We model $f(\mathbf{u})$ as a multivariate Gaussian distribution, $f_g(\mathbf{u}; \boldsymbol{\mu}, \Sigma)$, where $\boldsymbol{\mu} = \langle \mathbf{u} \rangle$ and $\Sigma = \langle \mathbf{u}' (\mathbf{u}')^{\mathrm{T}} \rangle$.

$$f_g(\mathbf{u}; \boldsymbol{\mu}, \Sigma) = \frac{1}{(2\pi)^{3/2} |\Sigma|^{1/2}} \exp\left(-\frac{1}{2} (\mathbf{u} - \boldsymbol{\mu})^{\mathrm{T}} \Sigma^{-1} (\mathbf{u} - \boldsymbol{\mu}) \right) \tag{9}$$

Using this function, we obtain an estimate of V_{ms}, $V_{\mathrm{ms,g}}$.

$$V_{\mathrm{ms,g}} = \int_{\Omega} s f_g(\mathbf{u}; \boldsymbol{\mu}, \Sigma) \mathrm{d}\mathbf{u} \tag{10}$$

Because Eq. (10) cannot be evaluated analytically, we implemented it to a code so it can be numerically integrated.

Results of the estimation of V_{ms}

Fig. 8 shows correlation between V_{ms} and $V_{\mathrm{ms,v}}$, and V_{ms} and $V_{\mathrm{ms,g}}$. We define mean bias (MB), mean ratio (MR) and mean normalized gross error (MNGE) in Eq. (11).

$$\mathrm{MB} = \frac{1}{M} \sum_{i=1}^{M} \left(V_{(i)} - V_{\mathrm{ms}(i)} \right) \tag{11a}$$

$$\mathrm{MR} = \frac{1}{M} \sum_{i=1}^{M} \frac{V_{(i)}}{V_{\mathrm{ms}(i)}} \tag{11b}$$

$$\mathrm{MNGE} = \frac{1}{M} \sum_{i=1}^{M} \left| \frac{V_{(i)} - V_{\mathrm{ms}(i)}}{V_{\mathrm{ms}(i)}} \right| \tag{11c}$$

Here, V represents a mean wind speed other than V_{ms}, i is a suffix that indicates the data point, and M is the total number of data points. Using these three indices, Table 3 summarizes the scores of the mean wind speeds in terms of their approximation to V_{ms}.

$V_{\mathrm{ms,v}}$ approached V_{ms} more closely than V_{mv} and V_{es} on average. However, $V_{\mathrm{ms,v}}$ tended to be smaller than V_{ms} and there were some points at which V_{es} was closer to V_{ms} than $V_{\mathrm{ms,v}}$. On the other hand, $V_{\mathrm{ms,g}}$ coincided with V_{ms} very well. The probability distribution of the instantaneous wind velocity is not necessarily the Gaussian distribution. Yet, the results showed that, in the flow analyzed in this study, the modeling of the probability distribution succeeded on producing estimates of V_{ms} with sufficient accuracy.

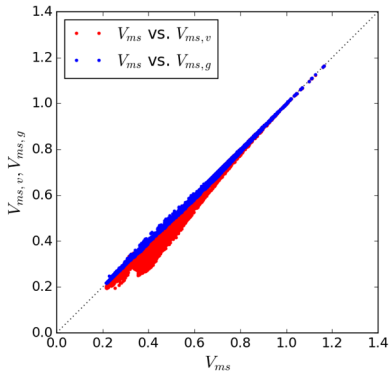

Figure 8. Scatter plot between exact and estimated V_{ms} in the range of -1 < x/H < 2, -1 < y/H < 1 and z/H = 1/16.

	V_{mv}	V_{es}	$V_{\mathrm{ms,v}}$	$V_{\mathrm{ms,g}}$
Mean bias (MB)	-0.068	0.027	-0.016	-0.001
Mean ratio (MR)	0.833	1.058	0.963	0.999
Mean normalized gross error (MNGE)	0.167	0.058	0.037	0.006

Table 3. Metrics of mean wind speeds as estimates of V_{ms} in the range of -1 < x/H < 2, -1 < y/H < 1 and z/H = 1/16.

7. Conclusions

The relationships between the mean wind speeds using three different definitions (mean-vector speed, mean speed, and effective speed) used in PWE analysis were studied analytically. Furthermore, by conducting a LES of the flow around a single building model in the urban boundary layer, the discrepancies between the mean wind speeds were quantitatively analyzed. In the vicinity of the ground surface, the difference between the mean wind speeds became larger in the recirculation flow near the building's windward corners and in the wake of the building. However, in the region where the maximum wind speed occurred, all mean wind speeds showed values very similar to each other. Moreover, we presented methods to estimate the mean speed based on information obtained from CFD (RANS). By modeling the probability distribution of the instantaneous velocity vector in a multivariate Gaussian distribution, we demonstrated its ability to estimate the mean speed with high accuracy.

Acknowledgments

Part of this work was supported by the Japan Society for the Promotion of Science (JSPS) KAKENHI, grant number 26709041.

References

[1] Y. Tominaga, A. Mochida, T. Shirasawa, R. Yoshie, H. Kataoka, K. Harimoto, and T. Nozu, "Cross comparisons of CFD results of wind environment at pedestrian level around a high-rise building and within a building complex," *J. Asian Archit. Build. Eng.*, vol. 3, no. 1, pp. 63–70, 2004.

[2] Architectural Institute of Japan, *AIJ benchmarks for validation of CFD simulations applied to pedestrian wind environment around buildings*. Tokyo: Architectural Institute of Japan, 2016.

[3] Y. Tominaga, A. Mochida, S. Murakami, and S. Sawaki, "Comparison of various revised k–ε models and LES applied to flow around a high-rise building model with 1:1:2 shape placed within the surface boundary layer," *J. Wind Eng. Ind. Aerodyn.*, vol. 96, no. 4, pp. 389–411, Apr. 2008.